Electronic Supporting Information

Amphiphilic oligo(2-ethyl-2-oxazoline)s via straightforward synthesis and their self-assembly behaviour

James Lefley [a], Zivani Varanaraja [a], Ben Drain [a], Steven Huband [b], James Beament [c] and C. Remzi Becer [a*]

[a] *Department of Chemistry, University of Warwick, Coventry, CV4 7AL, United Kingdom*

[b] *X-ray Diffraction RTP, Department of Physics, University of Warwick, Coventry, CV4 7AL, United Kingdom*

[c] *Infineum UK Ltd., Milton Hill Business & Technology Centre, Abingdon, Oxfordshire OX13 6BB, United Kingdom*

** Corresponding author: Remzi.Becer@warwick.ac.uk*

Materials

2-Ethyl-2-oxazoline 99+% (Acros Organics, EtOx) was dried over calcium hydride and distilled under reduced pressure prior to use. Propargyl p-toluenesulfonate 98% (Aldrich, PropTos) was distilled under reduced pressure and stored under nitrogen. Extra dry acetonitrile 99+% was purchased from Acros Organics and stored over molecular sieves under an inert atmosphere. Azobisisobutyronitrile 98% (AIBN), 1-dodecanethiol ≥ 98%, piperidine (pip) and N,N-diisopropylethylamine ≥ 99% (DIPEA) and were all purchased from Sigma Aldrich and were used as received.

^{1}H Nuclear Magnetic Resonance (NMR)

All spectra were recorded on a Bruker Advance III HD 300 MHz. Purified products were recorded on a Bruker Advance III HD 400 MHz. $CDCl_3$ was used as the solvent and the signal

of the residual $CHCl_3$ served as reference for the chemical shift, δ. Data analysis was performed using TopSpin 3.2 software.

Gel Permeation Chromatography (GPC)

The measurements were performed using THF (2% TEA and 0.01% BHT) as the eluent. The Agilent Technologies 1260 Infinity instrument was equipped with a refractive index (RI) and 308 nm UV detectors, a PLgel 5 μm guard column, and a PLgel 5 μm mixed D column (300 × 7.5 mm). Samples were run at 1 mL min^{-1} at 40 °C. Poly(methyl methacrylate) standards (Agilent PMMA calibration kits, M-M-10 and M-L-10 MW range 500-120,000) were used for the calibration. Before injection (100 μL), the samples were filtered through a PTFE membrane with 0.2 μm pore size. The data was determined by conventional calibration using Agilent GPC/SEC software and plotted in OriginPro 2022b.

Matrix Assisted Laser Desorption Ionisation Time-of-Flight Mass Spectrometry (MALDI ToF MS)

All MALDI-TOF was performed on a Bruker Autoflex Speed mass spectrometer using a nitrogen laser delivering 2 ns pulses at 337 nm with positive ion ToF detection performed using an accelerating voltage of 25 kV. The matrix used was trans-2-[3-(4-tertbutylphenyl)-2-methyl2-propylidene]malonitrile (DCTB) dissolved in THF and sodium trifluoroacetate used as a S2 cationic agent (solution in ethanol). Samples were measured in reflective mode and calibrated against poly(methyl methacrylate) standards.

Differential Scanning Calorimetry (DSC)

Thermal transitions were determined on a Mettler-Toledo DSC1 equipped with an autosampler under nitrogen atmosphere with a flow of 50 mL min^{-1}. 40 μL aluminium pans with 5-15 mg of sample were prepared. Initial ramp from 25 °C to 200 °C at 50 °C min^{-1}, followed by quenching to -100 °C at -150 °C min^{-1}. Then, two heating and cooling cycles from -50 °C to

200 °C at a rate of 5°C min^{-1} was performed. The T_g value was calculated using Mettler-Toledo thermal analysis software, identified as a second order exothermic transition in the second heating curve.

Thermogravimetric Analysis (TGA)

The analyses were performed on a Mettler-Toledo TGA equipped with an autosampler under an air flow of 50 mL min−1 from 25 to 550 °C at a heating rate of 5 °C min^{-1}. 40 µL aluminium pans were used with 5-15 mg of sample. The degradation temperatures were reported as the onset temperature calculated using Mettler-Toledo thermal analysis software.

Dynamic Light Scattering (DLS)

Measurements were carried out on an Anton Paar Litesizer. A sample (2mL) of each oligomer nanoparticle solution was filtered through a 0.2µm PTFE filter and taken for measurement in a Suprasil quartz cuvette (Hellman, 100-QS, light path of 10.00 mm). Samples were measured at 25 ˚C at a backscattering measuring angle of 175˚. Each sample was measured in triplicate with 30 runs per measurement and 5 minutes equilibration time between each measurement. P(EtOx) refractive index used was 1.52.

Small Angle X-ray Scattering (SAXS)

Small-angle X-ray scattering (SAXS) measurements were made using a Xenocs Xeuss 2.0 equipped with a micro-focus Cu K_α source collimated with Scatterless slits. The scattering was measured using a Pilatus 300k detector with a pixel size of 0.172 mm x 0.172 mm. The distance between the detector and the sample was calibrated using silver behenate ($AgC_{22}H_{43}O_2$), giving a value of 1.196 (3) m. The magnitude of the scattering vector (q) is given by $q = 4\pi \sin\theta/\lambda$, where 2θ is the angle between the incident and scattered X-rays and λ is the wavelength of the incident X-rays. This gave a q range for the detector of 0.01 $Å^{-1}$ and 0.3 $Å^{-1}$.

An azimuthal integration of the 2D scattering profile was performed using Xenocs XSACT software and the resulting data corrected for the absorption, sample thickness and background. [1,2] SAXS pattern were collected at 25 °C for with four repeat one hour collections. These four measurements were then combined to produce a single file with a total counting time of four hours.

The SAXS data was modelled using a core-shell sphere model where the core radius was given by given by a Gaussian distribution. The width of the Gaussian distribution was fixed such that $\sigma/\mu = 0.05$, where σ is the standard deviation and μ is the mean radius. The SAXS response was modelled using SASview. [3] The scattering intensity in the cores-shell sphere model is calculated according to

$$P(q) = V_f F^2(q) + background$$

Where V_f is the volume fraction of particles F(q) is given by

$$F(q) = \frac{3}{V_s}\left[V_c(\rho_c - \rho_s)\frac{\sin(qr_c) - qr_c\cos(qr_c)}{(qr_c)^3} + V_s(\rho_s - \rho_{solv})\frac{\sin(qr_s) - qr_s\cos(qr_s)}{(qr_s)^3}\right]$$

Where V_s is the volume of the whole particle, V_c is the volume of the core, r_s is the core radius plus shell thickness, r_c is the core radius, ρ_c is the scattering length density (SLD) of the core, ρ_s is the SLD of the shell and ρ_{solv} is the SLD of the solvent. [4] The SLD values used for the modelling were calculated using the Irena SAS macros running in Igor Pro and are listed in Table S1. [5]

Table S1. Material and SLD values for modelling of SAXS data.

Material	Chemical formula	Density	SLD/x10^6/Å^2	Model
Dodecanethiol	$C_{12}H_{26}S$	0.845	8.076	Core
P(EtOx)$_{10}$	$C_{50}H_{90}O_{10}N_{10}$	1.140	10.16	Shell
DI water	H_2O	1.000	9.42	solvent

Sample **TF2**-loaded shows signs of agglomeration with an increase in the scattering at low q values. To model this a power law slope of the form $I(q) = scale * q^{-P}$. Where P is fixed to a value of 4 which follows the Porod law. [6]

The measured SAXS data and the fits to the scattering are plotted in **Fig 3**. The fit parameters are listed in **Table S2**. The SAXS response from these samples is relatively weak so the fitting range has been chosen to avoid the regions at low q values with large uncertainties. The scattering from agglomerated particles causes the increase in scattering at low q values.

Table S2. Fit parameters of SAXS modelling using a core-shell sphere model.

Sample	Mean core radius (Å)	Mean shell thickness (Å)	Vol. fraction/%	Agglom.
TF1-UL	16.6(1)	19.7(4)	0.55	No
TF1-L	15.2(5)	23(1)	0.19	No
TF2-L	20.4(1)	26.0(2)	0.53	No
TF2-UL	18.4(1)	26.3(2)	0.67	Yes

Transmission Electron Microscopy (TEM)

TF1 and **TF2** were selected for TEM imaging. 10 mg/ml nanoparticle solutions were imaged after a negative staining treatment. The samples were drop-casted on glow discharged 300 mesh carbon-coated copper TEM grids (Agar Scientific, Stansted, U.K.). After 3 minutes incubation, excess solution was removed by blotting with filter paper before incubation with 0.75% phosphotungstic acid solution for 1 minute. Excess stain was removed by blotting with filter paper and dried under vacuum before imaging. Bright-field TEM imaging was performed on a JEOL 2100 Plus Transmission Electron Microscope operated at an acceleration voltage of 200 kV. All the images were recorded on a Gatan Orius 11 megapixel digital camera and at least six areas were analysed.

UV-Vis Spectroscopy

Agilent Technologies Cary 100 UV-Vis spectrophotometer equipped with an Agilent Technologies Cary temperature controller and An Agilent Technologies 6 x 6 multicell block Peltier was used for constructing the calibration curve and quantifying the mass of encapsulated curcumin for each oligomer. The measurements were performed using the Suprasil quartz cuvettes (Hellman, 100-QS, light path of 10.00 mm) filled with 10 mg/mL nanoparticle solutions. A single scan was performed at 25 °C between the wavelengths 200nm – 800nm. Absorbance values for each sample were taken at wavelength λ_{max} = 428 nm. For turbidimetry studies, thermal scans were recorded at a wavelength of 600 nm between 20-60˚C at a heating rate of 0.5 ˚C/min whilst taking a data recordings at 1.0˚C increments. Cloud point temperatures (T_{cp}) were determined at 50% transmittance. C_{oligo} = 10 mg/ml and C_{CUR} = 2 mg/ml. All the data was obtained using the Cary WinUV software and plotted using the OriginPro 2022b.

Synthesis of TF0 ($P(EtOx)_{10}$-Pip)

EtOx (2.00 g, 20.18 mmol, 10 eqv), PropTos (0.35 mL, 2.018 mmol, 1 eqv) and acetonitrile (5.00 mL) were added to a sealed microwave vial with stirrer bar and degassed with N_2 for 15 minutes. A small aliquot was taken to calculate [M]:[I] via ^{1}H NMR. The vial was then placed in an oil bath and the reaction proceeded for 30 minutes at 110 ˚C stirring at 600 rpm. After 30 mins, the heat was reduced to 25 ˚C. A relief needle was inserted into the seal to release the pressure from the vial and a small aliquot was taken for monomer conversion and molecular weight analysis. Piperidine (10.09 mmol, 1.00 mL, 5 eqv) was added to terminate the reaction and the reaction mixture was allowed to stir for 18 hours at 25 ˚C. The reaction mixture was precipitated twice into cold ether, filtered and dried under reduced pressure to yield the product $PEtOx_{10}$-pip (1.71 g, white powder). From **Fig S1A**, the ratio of [M]:[I] was calculated as 11:1.

According to the ^{1}H NMR spectrum of the purified product (**Fig. S1B**), the actual ratio is [M]:[I] = 10:1.

Synthesis of TF1 ($P(EtOx)_{10}$-S-C_{12})

Same procedure used for the synthesis of **TF0** but instead of piperidine, 1-dodecanethiol (10.09 mmol, 2.42 mL, 5 eqv) and DIPEA (10.09 mmol, 1.76 mL, 5 eqv) were added to terminate the reaction. The reaction mixture was precipitated twice into cold ether, filtered and dried under reduced pressure to yield the product $PEtOx_{10}$-S-C_{12} (1.39 g, pale yellow tacky solid).

Synthesis of TF2 ($P(EtOx)_{10}$-$(S-C_{12})_2$)

Same procedure used for the synthesis of **TF0**. The reaction mixture was precipitated twice into cold ether, filtered and dried under reduced pressure to yield the intermediate product $PEtOx_{10}$-pip (1.65 g, white powder).

$PEtOx_{10}$-pip (1.48 mmol, 1.65 g, 1 eqv), AIBN (0.37 mmol, 61 mg, 0.25 eqv), dodecanethiol (7.40 mmol, 1.76 mL, 5 eqv) and acetonitrile (4 mL) and was added to a sealed microwave vial with a stirrer bar and degassed with N_2 for 15 minutes. The vial was then placed in an oil bath and the reaction proceeded for 24 hours at 70 ˚C stirring at 600 rpm. A relief needle was inserted into the seal to release the pressure from the vial. The reaction mixture was precipitated twice into cold ether, filtered and dried under reduced pressure to yield the product $PEtOx_{10}$-$(S-C_{12})_2$ (0.82 g, pale yellow powder).

Synthesis of TF3 ($P(EtOx)_{10}$-$(S-C_{12})_3$)

Same procedure used for the synthesis of **TF1**. After adding dodecanethiol and DIPEA and leaving to stir for 18 hours, the reaction vial was degassed with nitrogen for 15 minutes and heated to 70 ˚C. Meanwhile, AIBN (0.50 mmol, 83 mg, 0.25 eqv) was dissolved in acetonitrile (1 mL), degassed for 15 minutes and was added to the reaction mixture and left to stir for 24

hours. A relief needle was inserted into the seal to release the pressure from the vial. The mixture was then precipitated twice into cold hexane, filtered and dried under reduced pressure to yield the product $PEtOx_{10}$-$(S\text{-}C_{12})_3$ (1.09 g, yellow tacky solid).

Preparation of nanoparticles via thin film hydration

Modified from literature.[7] 30 mg of oligomer was dissolved in 1 mL of ethanol and was added to a 20 mL scintillation vial. The vial was placed in a heating block set to 50 ˚C and the ethanol was evaporated under a flow of nitrogen to form a thin film. The vial containing the film was placed in a vacuum oven for 24 hours prior to rehydration. 3 mL of Mili-Q® deionised water was added to the vial and stirred (600rpm) at 25 ˚C for 24 hours. The nanoparticle solution was filtered using a 0.22 µm Nylon syringe filter ready for further analysis.

Preparation of nanoparticles via nanoprecipitation

Modified from literature.[8] 30 mg of oligomer was dissolved in 1 mL of THF. The oligomer/THF solution was then added dropwise to a vial containing 3 mL of Mili-Q® deionised water stirring at 600 rpm using a New Era NE-1000 Syringe Pump set to deliver the solution at a rate of 1 mL/min. The solution was allowed to stir for 10 minutes before being placed in an oil bath set at 25 ˚C. The lid was left off and the THF was allowed to evaporate over 4 hours. Removal of THF was confirmed by ^{1}H NMR. The nanoparticle solution was stirred for a further 24 hours and was filtered using a 0.22 µm Nylon syringe filter ready for further analysis.

Preparation of curcumin-loaded nanoparticles via thin film hydration

Modified from literature.[7] Stock solutions of oligomer (3 mL, 10 mg/ml) and curcumin (0.6 mL, 1.2 mL and 2.4 mL, 5 mg/ml) in ethanol were mixed in the desired ratios and added to

separate 20 mL scintillation vials. Vials were placed in a heating block set to 50 ˚C and the ethanol was evaporated under a flow of nitrogen to form the thin films. Films were placed in a vacuum oven for 24 hours prior to rehydration. 3 mL of Mili-Q® deionised water was added to each vial and stirred (600rpm) at 25 ˚C for 24 hours. The nanoformulations were centrifuged (7500 rpm, 10 minutes) and filtered (0.22 µm Nylon) to remove any non-solubilized curcumin. A 50 µL aliquot was taken from each nanoformulation and diluted with 950 µL ethanol to form a 20-fold dilution. In the case of TF2, 50 µL was taken and diluted in 1950 µL to form a 40-fold dilution due to the high concentration of CUR solubilized. The amount of solubilized curcumin was calculated by UV-Vis Spectroscopy using the calibration curve and the absorbance value at λ_{max} = 428 nm to determine the concentration of curcumin. Nanoformulations were stored at 4 ˚C and analysed 6 months later. Samples were centrifuged and filtered prior to measurements to remove any free, non-encapsulated curcumin.

Determination of critical micelle concentration via pyrene fluorescence spectroscopy

Procedure taken from literature.[9] A stock solution of pyrene in acetone (2.5×10^{-5} mol/L) was prepared. 60 µL of this stock solution was each added to an empty vial and the acetone was allowed to evaporate under gentle heat and air flow. A variety of oligomer solutions ranging from 10 mg/mL to 10^{-7} mg/mL were prepared by serial dilution. To each vial containing the dried pyrene, one of the oligomer solutions was added, closed, and stirred for 24 h at 25 ˚C. The fluorescence spectrum was then recorded for each sample. The fluorescence spectra were recorded on an Agilent Cary Eclipse Fluorescence Spectrophotometer (right angle geometry 1 cm x 1 cm quartz cuvette) using the following conditions: excitation at 334 nm, slit width 2.5 nm for excitation and 5 nm for emission. Spectra measured between 350 nm and 500 nm. The ratio (I_1/I_3) of the intensities of the vibrational bands at 372 nm (I_1) and 391 nm (I_3) were plotted against oligomer concentration. The cmc was determined as the intersection between the two tangents of the plot.

Calculation of Encapsulation Efficiency and Drug Loading Capacity

$$Loading\ Efficiency\ (LE\%) = \frac{m_{CUR}}{m_{CUR\ added}} \times 100 \qquad \textbf{Eq 1}$$

Where m_{CUR} is the mass of the encapsulated curcumin and $m_{CUR\ added}$ is the mass of the initial curcumin added in the feed.

$$Drug\ Loading\ Capacity\ (DL\%) = \frac{m_{CUR}}{m_{CUR} + m_{oligomer}} \times 100 \qquad \textbf{Eq 2}$$

Where m_{CUR} is the mass of the encapsulated curcumin and $m_{polymer}$ is the mass of the oligomer.

TF0 ($PEtOx_{10}$-Pip)

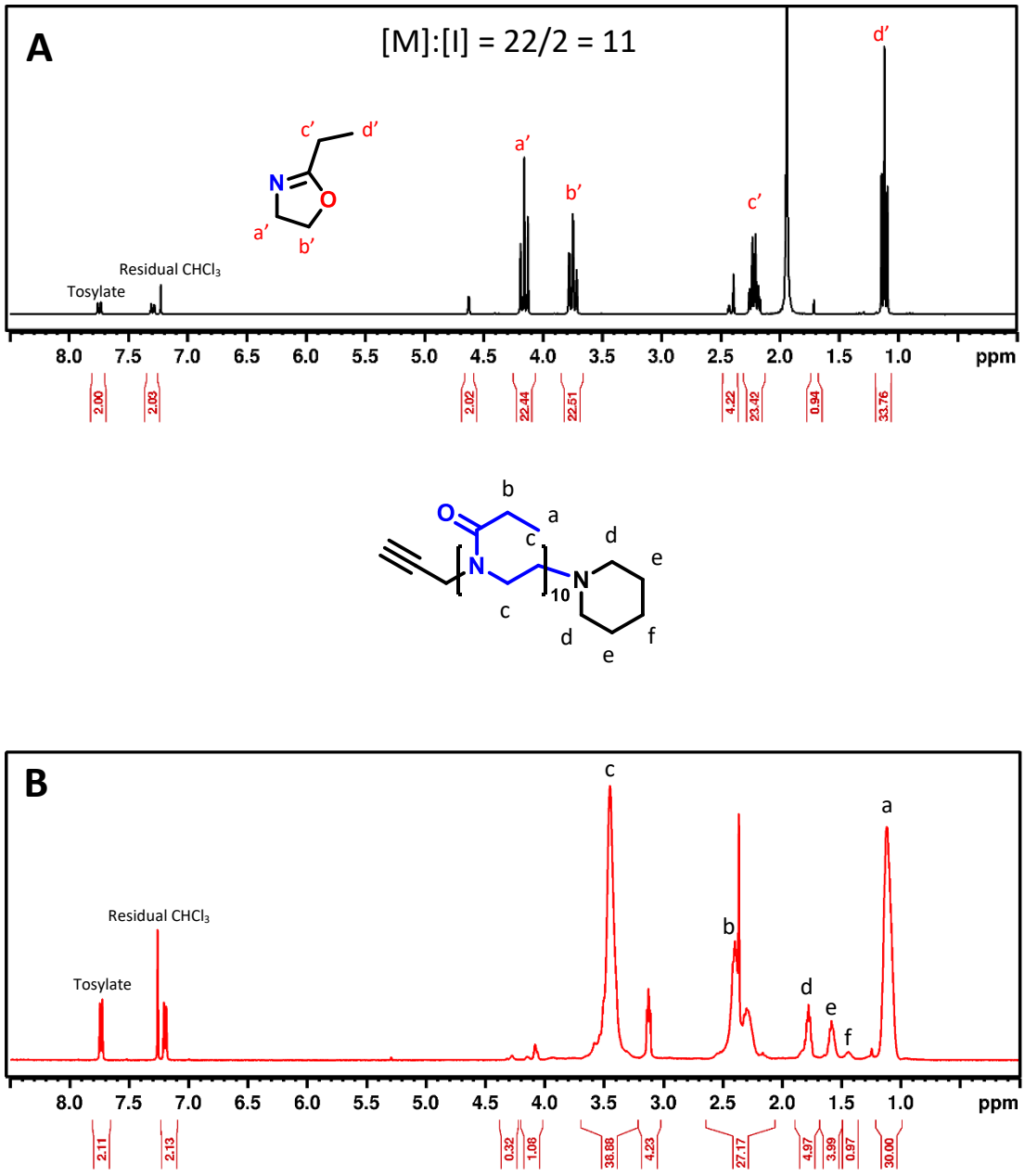

Figure S1. Partially assigned ^{1}H NMR spectra of TF0 before polymerization (A) and the pure product after endcapping and precipitation (B).

^{1}H NMR (400 MHz, $CDCl_3$, 298K) δ (ppm): 3.71-3.22 (br, 40H, H^{c}), 2.6-2.08 (br, 28H, H^{b}), 1.78 (m, 4H, H^{d}), 1.58 (m, 4H, H^{e}), 1.5-1.37 (br, 1H, H^{f}), 1.20-1.00 (br, 31H, H^{a})

$M_{n,\,NMR}$ = 1.1 kDa

SEC (THF, RI detector, PMMA calibration): M_n = 1.7 kDa , $Đ$ = 1.08

TF1 ($PEtOx_{10}$-S-C_{12})

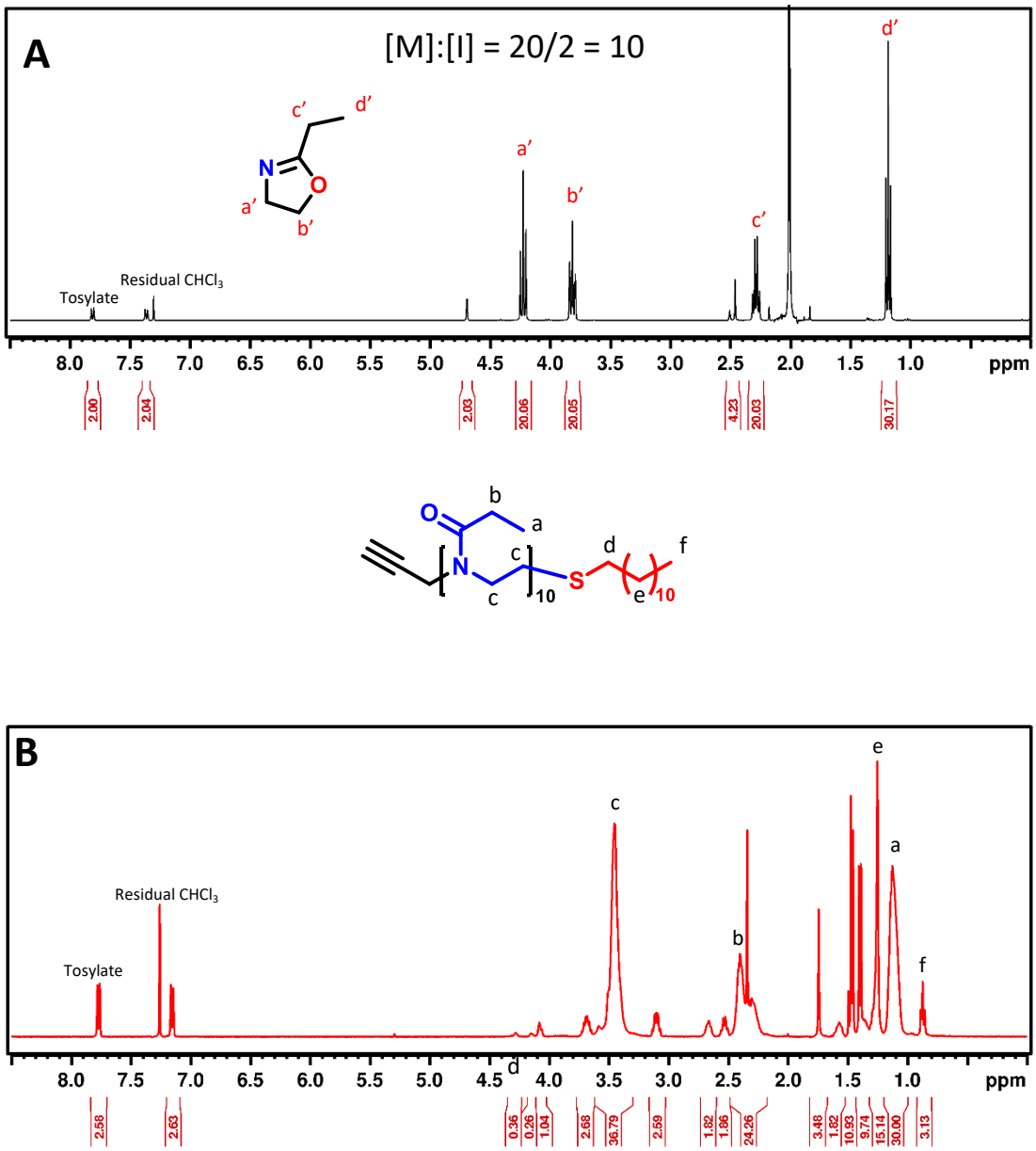

Figure S2. Partially assigned ^{1}H NMR spectra of TF1 before polymerization (A) and the pure product after endcapping and precipitation (B).

^{1}H NMR (400 MHz, $CDCl_3$, 298K) δ (ppm): 3.62-3.33 (br, 37H, H^{c}), 2.53 (q, 2H, H^{d}), 2.49-2.20 (br, 24H, H^{b}), 1.32-1.2 (br, 15H, H^{e}), 1.20-1.10 (br, 30H, H^{a}), 0.90 (t, 3H, H^{f})

$M_{n,\,NMR}$ = 1.2 kDa

SEC (THF, RI detector, PMMA calibration): M_n = 2.0 kDa , $Đ$ = 1.10

TF2 ($PEtOx_{10}$-$(S\text{-}C_{12})_2$)

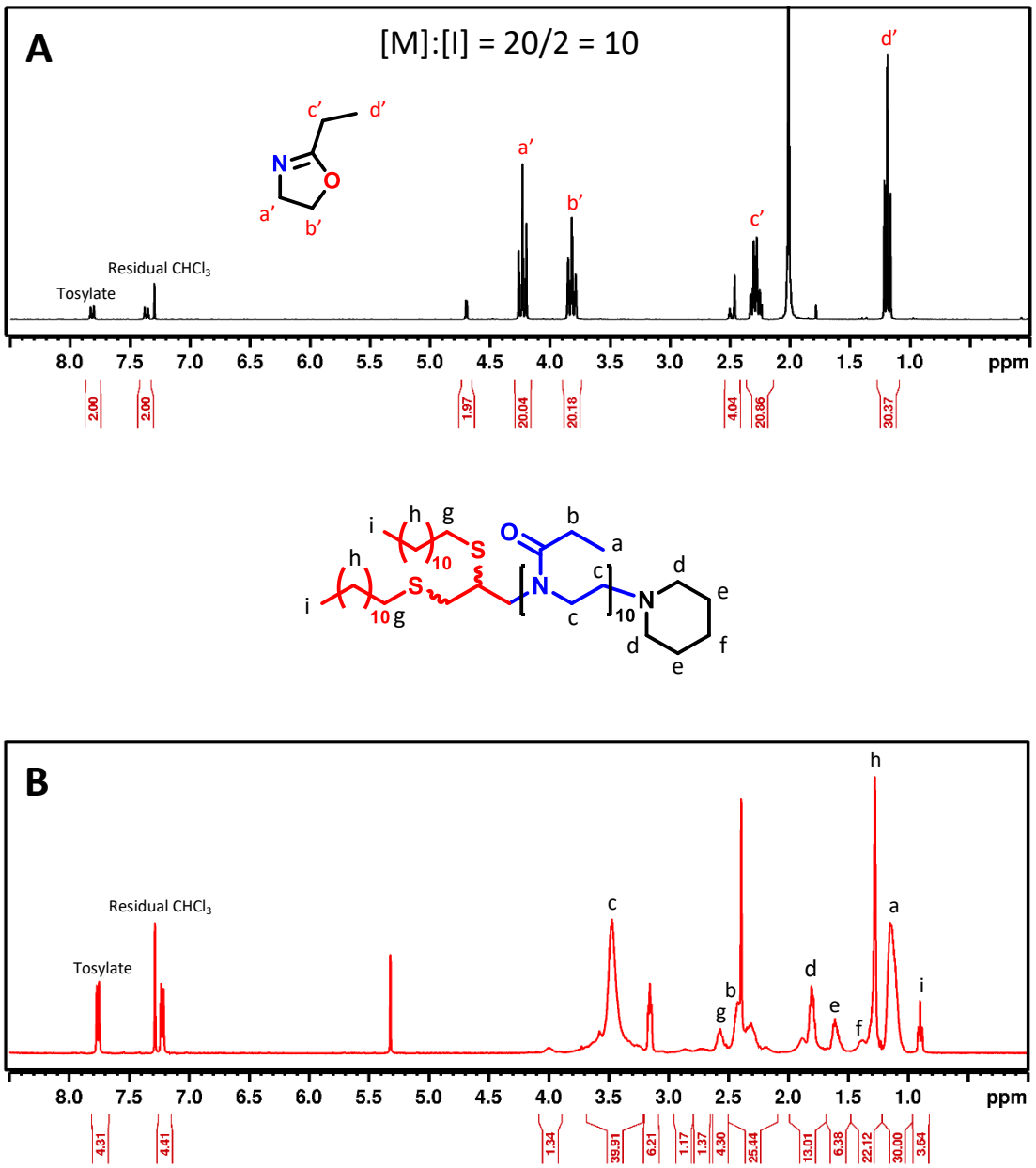

Figure S3. Partially assigned ^{1}H NMR spectra of TF2 before polymerization (A) and the pure product after endcapping and precipitation (B).

^{1}H NMR (400 MHz, $CDCl_3$, 298K) δ (ppm): 3.80-3.20 (br, 41H, H^{c}), 2.61-2.50 (br, 1H, H^{g}), 2.50-2.20 (br, 24H, H^{b}), 1.85-1.71 (br, 10H, H^{d}), 1.68-1.49 (br, 6H, H^{e}), 1.46-1.23 (br, 22H, H^{f+h}), 1.20-1.10 (br, 30H, H^{a}), 0.90 (t, 4H, H^{i})

$M_{n,\,NMR}$ = 1.5 kDa

SEC (THF, RI detector, PMMA calibration): M_n = 2.3 kDa , $Đ$ = 1.13

TF3 ($PEtOx_{10}$-$(S\text{-}C_{12})_3$)

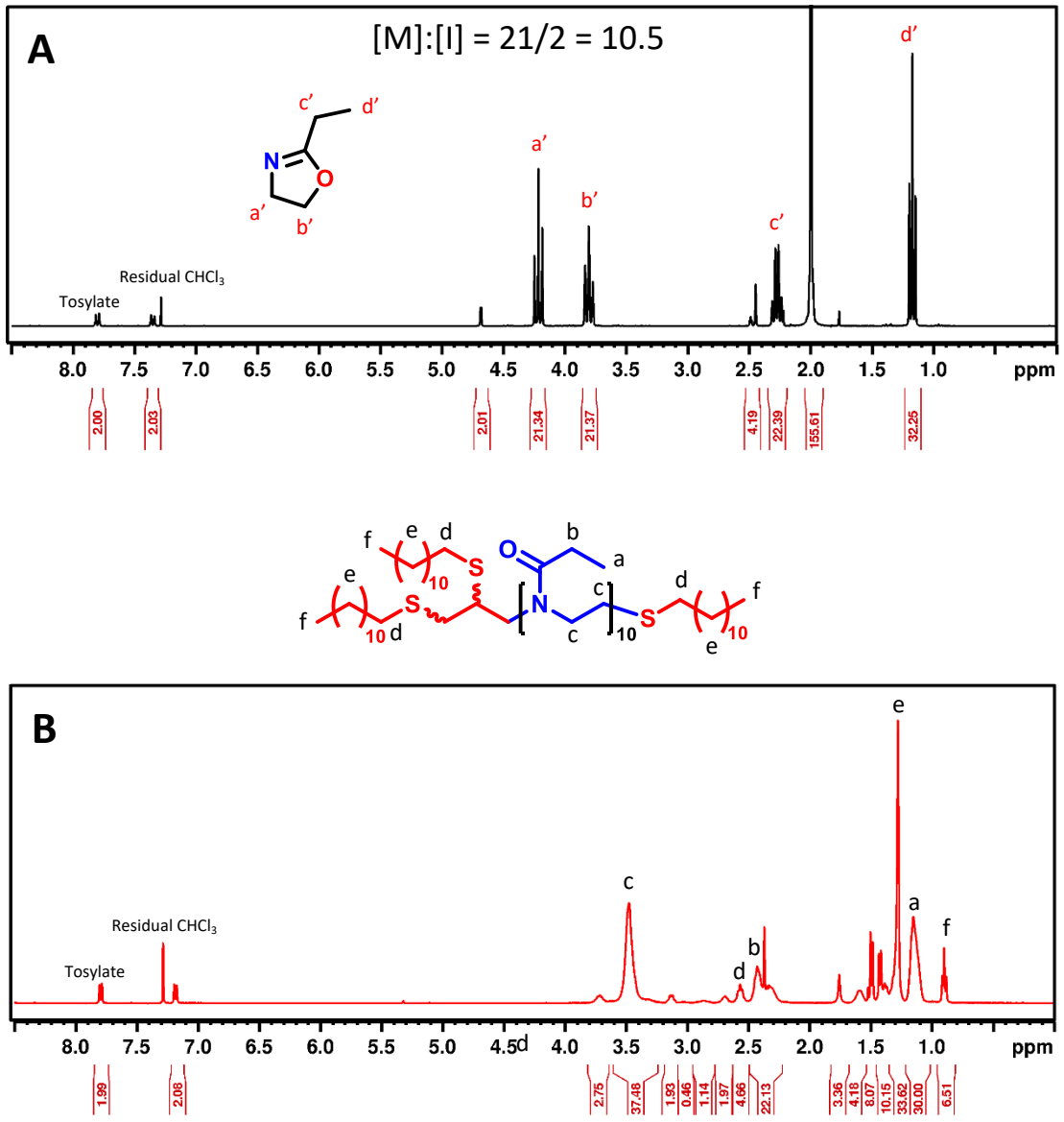

Figure S4. Partially assigned ^{1}H NMR spectra of TF3 before polymerization (A) and the pure product after endcapping and precipitation (B).

^{1}H NMR (400 MHz, $CDCl_3$, 298K) δ (ppm): 3.61-3.24 (br, 37H, H^{c}), 2.63-2.50 (m, 5H, H^{d}), 1.35-1.22 (br, 37H, H^{e}), 1.20-1.10 (br, 30H, H^{a}), 0.90 (t, 7H, H^{f})

$M_{n,\,NMR}$ = 1.6 kDa

SEC (THF, RI detector, PMMA calibration): M_n = 2.4 kDa , $Đ$ = 1.1

Table S3. Found and calculated m/z values of an individual n-mer of each oligomer **TF0**-**TF3** from the MALDI-ToF Spectra in Figure 2.

Sample	n-mer	[M+Na] found (Da)	[M+Na] calculated (Da)	Difference (Da)
TF0	13	1434.570	1434.884	0.314
TF1	13	1553.145	1552.134	1.011
TF2	11	1640.422	1640.432	0.010
TF3	12	1857.648	1856.812	0.836

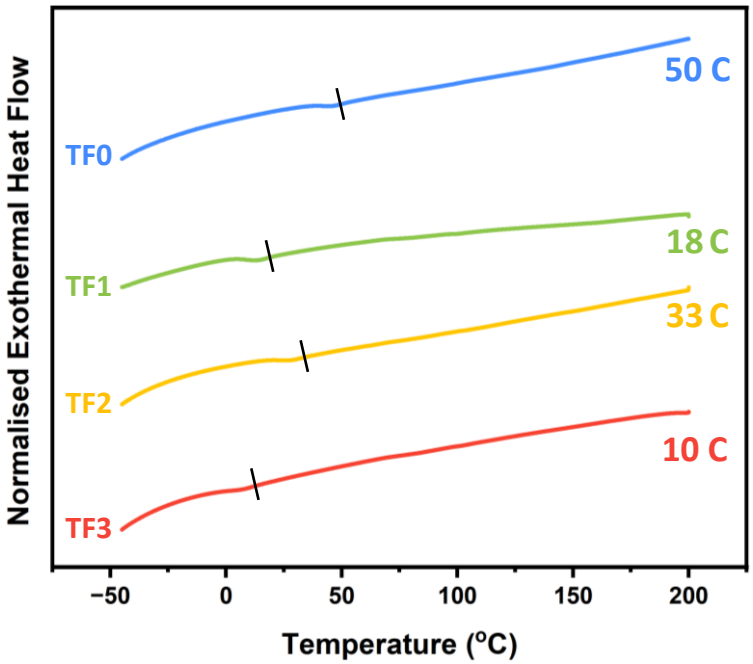

Figure S5. DSC thermograms of the 2nd heating cycle of dodecyl-functionalized PEtOx oligomers TF0-TF3. Measurements performed using a heating rate at 5 ˚C/min with each cycle ranging from -50 to 200 ˚C. Glass transition temperatures calculated from the inflection point of the curve and are marked as black dashes on the thermograms.

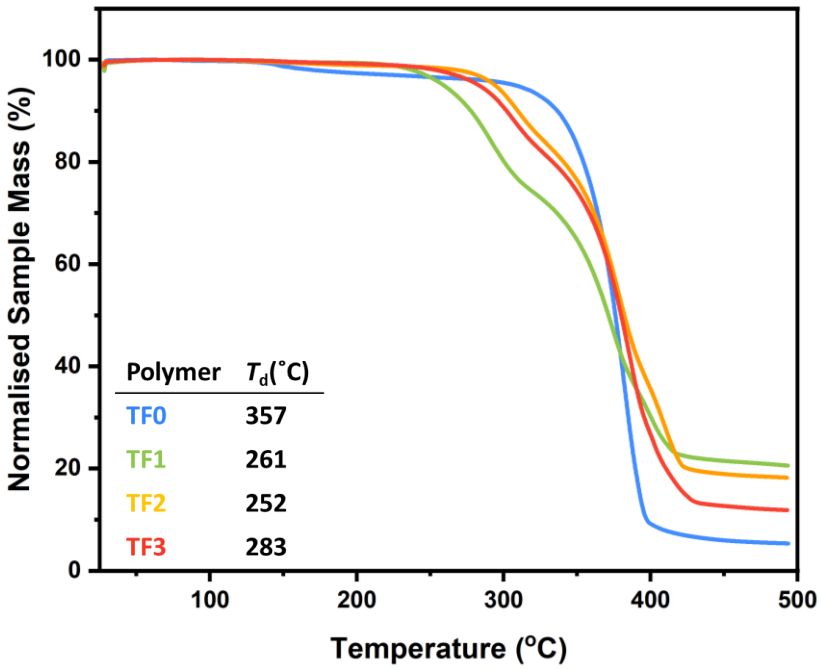

Figure S6. TGA thermograms of the dodecyl-functionalized PEtOx oligomers **TF0-TF3**. Measurements performed using a heating rate at 5 ˚C/min ranging from 25 to 500 ˚C. Degradation temperatures (T_d) are reported as the onset of degradation and were calculated using Mettler-Toledo thermal analysis software.

TF2 Batch Repeat Data

From t_0 [M]:[I] = 10:1

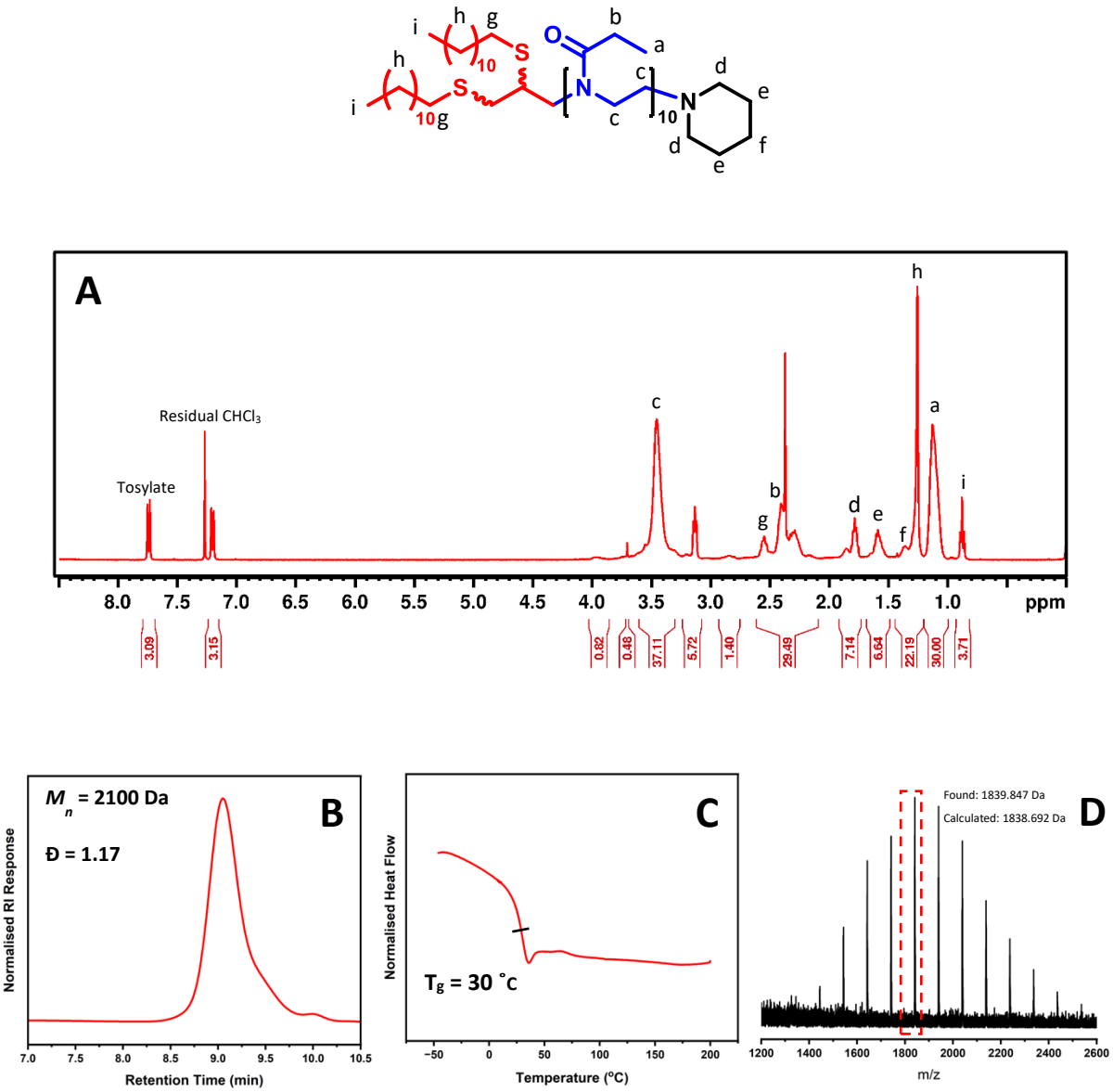

Figure S7. Characterisation data of the repeat batch of TF2 including spectra from ^{1}H NMR (A), GPC (B), DSC (C) and MALDI-ToF (D) analysis.

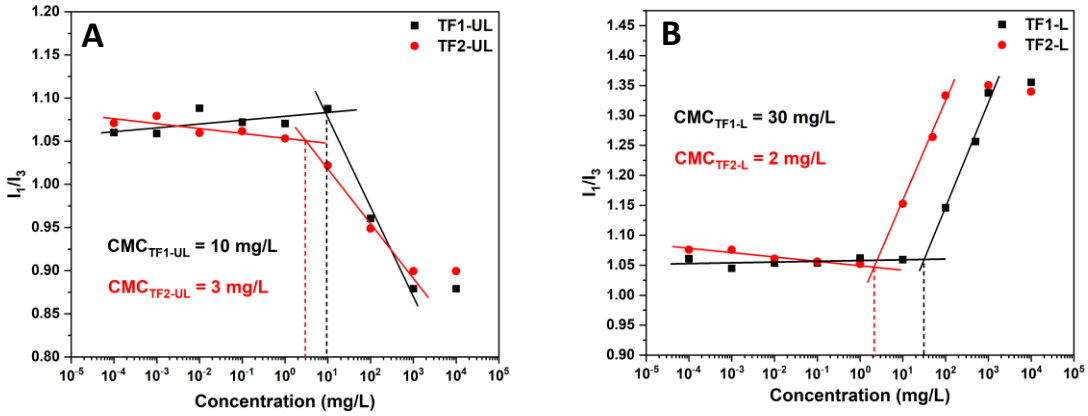

Figure S8. Determination of critical micelle concentrations (CMC) of **TF1** and **TF2** unloaded (A) and loaded (B) micelles via pyrene fluorescence spectroscopy where the ratio of I_1/I_3 (I_1 = 372 nm and I_3 = 391 nm) was plotted as a function of oligomer concentration. CMC values were determined as the intersection of the two tangents and indicated by the dashed lines.

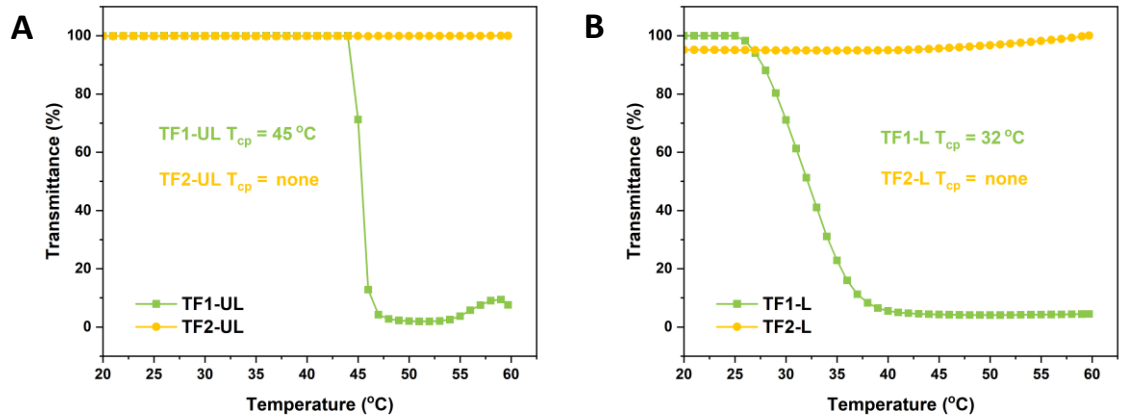

Figure S9. Turbidimetry measurements of TF1 and TF2 (A) unloaded and (B) loaded micelles measured between 25 ˚C and 60 ˚C with a heating rate of 0.5 ˚C/min. Cloud point temperatures (T_{cp}) determined at 50% transmittance. C_{oligo} = 10 mg/ml and C_{CUR} = 2 mg/ml.

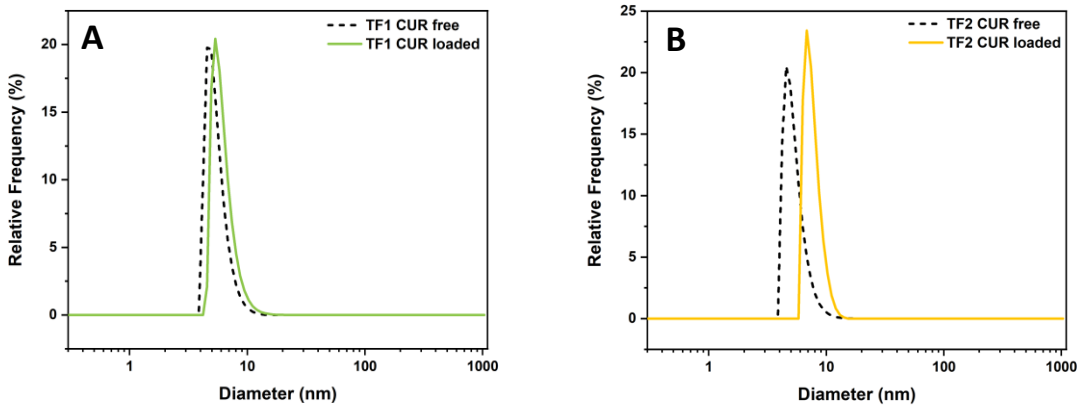

Figure S10. Number weighted DLS traces of TF1 (A) and TF2 (B) showing the curcumin loaded and curcumin free nanoparticles sizes. Measurements performed at 25 ˚C in Mili-Q deionised water. C_{oligo} = 10 mg/ml and C_{CUR} = 2 mg/ml.

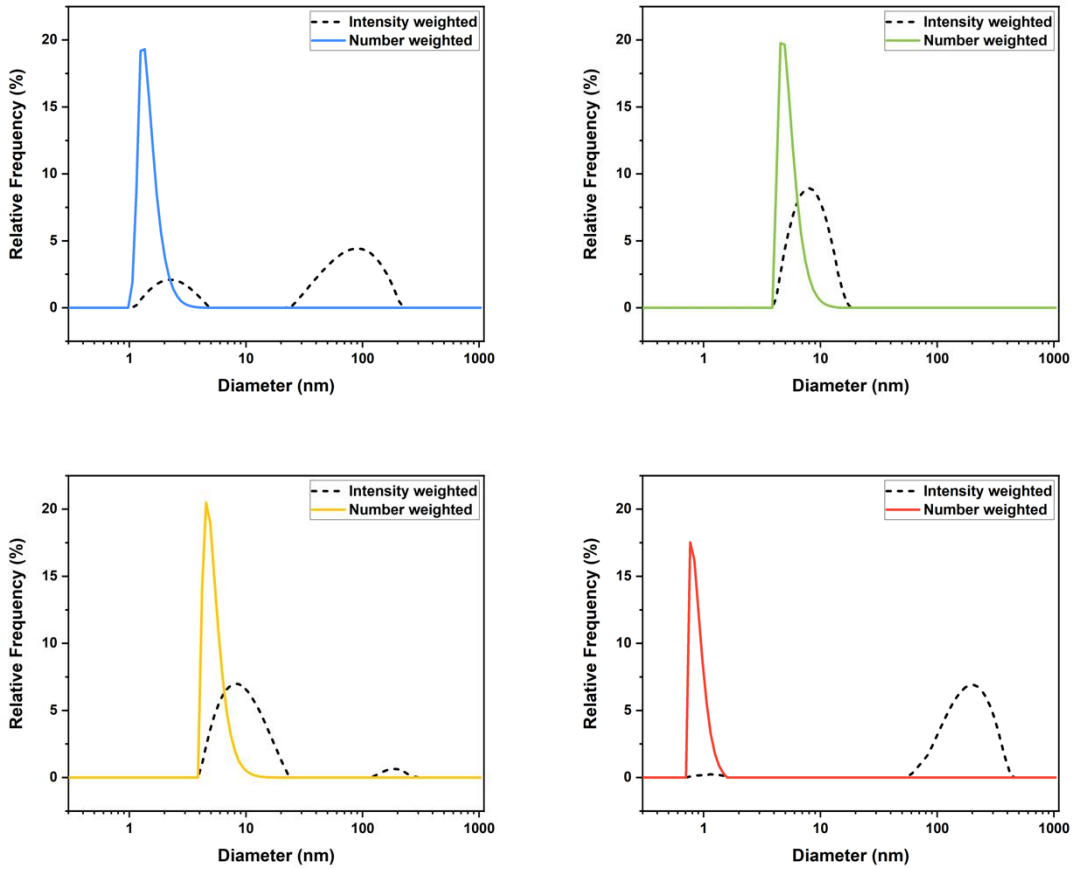

Figure S11. Intensity and number weighted DLS traces of TF0 (A), TF1 (B), TF2 (C) and TF3 (D) showing curcumin free nanoparticles sizes. Measurements performed at 25 ˚C in Mili-Q deionised water. C_{oligo} = 10 mg/ml and C_{CUR} = 2 mg/ml.

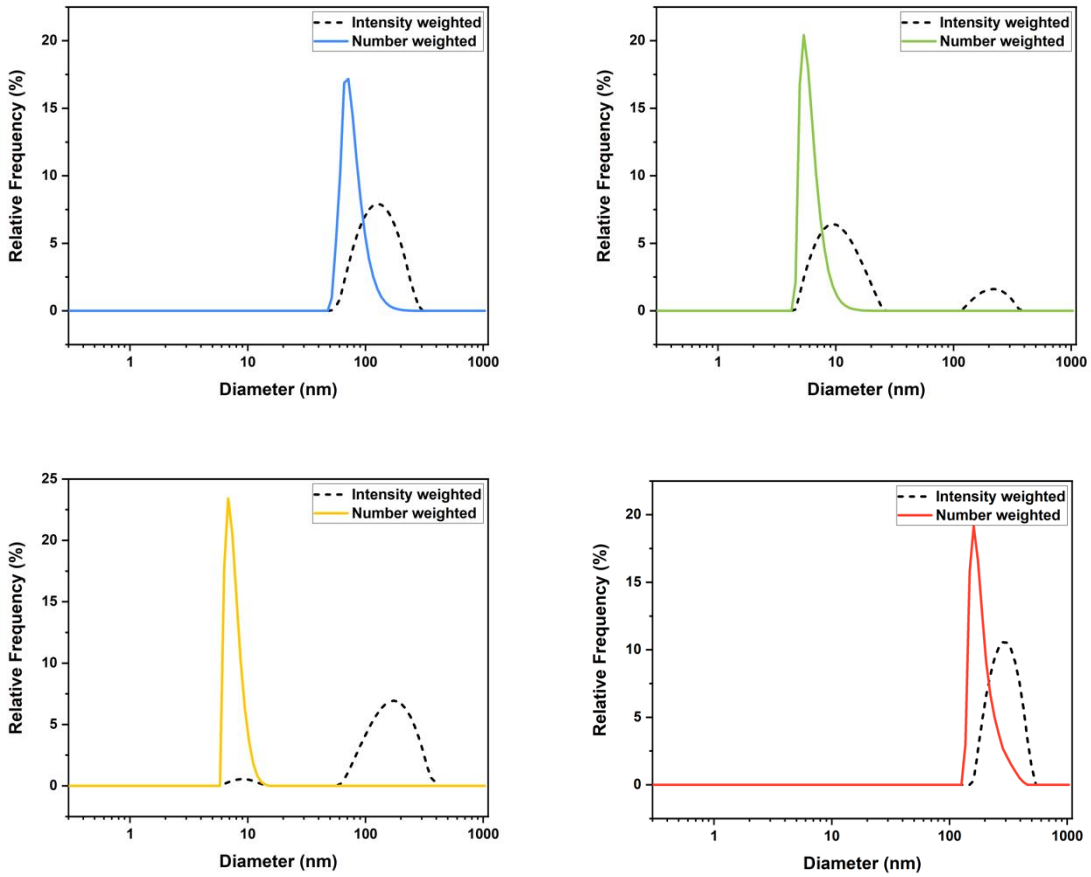

Figure S12. Intensity and number weighted DLS traces of TF0 (A), TF1 (B), TF2 (C) and TF3 (D) after encapsulation of curcumin via thin film hydration. Measurements performed at 25 ˚C in Mili-Q deionised water. C_{oligo} = 10 mg/ml and C_{CUR} = 2 mg/ml.

Table S4. Number averaged sizes of TF0-TF3 before and after encapsulation of curcumin via thin film hydration obtained by DLS. Measurements performed at 25 ˚C in Mili-Q deionised water. C_{oligo} = 10 mg/ml and C_{CUR} = 2 mg/ml.

Sample	**Curcumin free**		**Curcumin loaded**	
	Diameter (nm)	**PDI**	**Diameter (nm)**	**PDI**
TF0	1.50	0.31	79.20	0.20
TF1	5.47	0.11	6.82	0.22
TF2	5.39	0.21	7.65	0.23
TF3	1.17	0.24	192.37	0.24

Table S5. Encapsulation data of TF0-TF3 showing the amount of curcumin encapsulated, encapsulation efficiency (EE) and drug loading (DL) capacity of each oligomer using thin film hydration. Values expressed as mean ± SD (n=3). C_{oligo} = 10 mg/ml and C_{CUR} = 1, 2 and 4 mg/ml. Values determined from UV-Vis absorbance.

Sample	**Curcumin feed (mg/mL)**	**Solubilised CUR (mg/mL)**	**EE (%)**	**DL (%)**
TF0	1	0.019 ± 0.002	1.9 ± 0.2	0.19 ± 0.007
	2	0.016 ± 0.0004	0.8 ± 0.02	0.16 ± 0.004
	4	0.013 ± 0.0008	0.33 ± 0.02	0.13 ± 0.008
TF1	1	0.244 ± 0.058	24.4 ± 5.8	2.39 ± 0.58
	2	0.295 ± 0.039	14.75 ± 1.95	2.86 ± 0.38
	4	0.006 ± 0.002	0.15 ± 0.05	0.06 ± 0.02
TF2	1	0.635 ± 0.079	63.5 ± 7.9	5.97 ± 0.78
	2	0.828 ± 0.051	41.4 ± 2.55	7.65 ± 0.50
	4	0.346 ± 0.085	8.65 ± 3.06	3.34 ± 085
TF3	1	0.005 ± 0.002	0.5 ± 0.2	0.05 ± 0.02
	2	0.004 ± 0.002	0.2 ± 0.1	0.04 ± 0.02
	4	0.005 ± 0.003	0.13 ± 0.08	0.05 ± 0.03

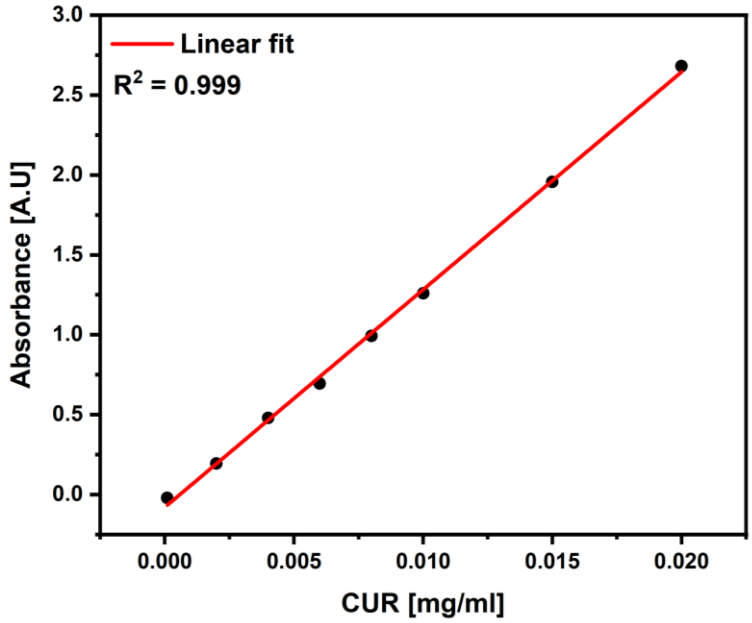

Figure S13. UV-Vis calibration curve constructed from known concentrations of curcumin with corresponding line of best fit. λ_{max} = 428 nm.

References:

1. Xenocs, "XSACT: X-ray Scattering Analysis and Calculation Tool." xsact.xenocs.com, 2021. SAXS & WAXS data analysis software — Version 2.4.
2. Fan Zhang, Jan Ilavsky, Gabrielle Long, John Quintana, Andrew Allen, and Pete Jemian, "*Glassy Carbon as an Absolute Intensity Calibration Standard for Small-Angle Scattering*," Metallurgical and Materials Transactions A 41 (5), 1151-1158 (2010).
3. M. Doucet et al. SasView Version 5.0.5, Zenodo, 10.5281/zenodo.6331344
4. A Guinier and G Fournet, *Small-Angle Scattering of X-Rays*, John Wiley and Sons, New York, (1955)
5. J. Ilavsky and P.R. Jemain, J Appl Crystallogr, 42, 347-353 (2009)
6. G Porod. *Kolloid Zeit*. 124 (1951) 83
7. M. M. Lübtow, L. Hahn, M. S. Haider and R. Luxenhofer, *Journal of the American Chemical Society*, 2017, **139**, 10980-10983
8. S. A. Meeuwissen, S. M. C. Bruekers, Y. Chen, D. J. Pochan and J. C. M. van Hest, *Polymer Chemistry*, 2014, **5**, 489-501
9. O. Colombani, M. Ruppel, F. Schubert, H. Zettl, D. V. Pergushov and A. H. E. Müller, *Macromolecules*, 2007, **40**, 12, 4338-4350